 doi:10.20944/preprints202209.0275.v1

Towards Building a Naturalistic Cycling Dataset Capturing Bicycle/Car Interactions

Fahd Alazemi
Graduate Research Assistant
Center for Sustainable Mobility
Virginia Tech Transportation Institute, Blacksburg, Virginia 24061
Email: falazemi@vt.edu

Karim Fadhloun, Ph.D.
Postdoctoral Associate
Center for Sustainable Mobility
Virginia Tech Transportation Institute, Blacksburg, Virginia 24061
Email: karim198@vt.edu

Hesham A. Rakha, Ph.D., P.Eng. (Corresponding author)
ORCiD: https://orcid.org/0000-0002-5845-2929
Samuel Reynolds Pritchard Professor of Engineering and Director
Center for Sustainable Mobility
Virginia Tech Transportation Institute, Blacksburg, Virginia 24061
Email: hrakha@vt.edu

Archak Mittal, Ph.D.
ORCiD: https://orcid.org/0000-0001-6186-4513
Research Scientist
Ford Motor Company
20000 Rotunda Drive
Dearborn, Michigan 48124
Email: amittal9@ford.com

Keywords: Bicycle Behavior, Naturalistic Cycling Data, Car/Bike Interactions, Computer Vision, Object Detection

 doi:10.20944/preprints202209.0275.v1

ABSTRACT

As machine learning and computer vision techniques and methods continue to advance, the collection of naturalistic traffic data from video feeds is becoming more and more feasible. That is especially true for the case of bicycles, for which the collection of naturalistic data is not achievable in the traditional vehicle approach. This study describes a research effort that aims to extract naturalistic cycling data from a video dataset for use in safety and mobility applications. The used videos come from a dataset collected in a previous Virginia Tech Transportation Institute study in collaboration with SPIN in which continuous video data at a non-signalized intersection on the Virginia Tech campus was recorded. The research team applied computer vision and machine learning techniques to develop a comprehensive framework for the extraction of naturalistic cycling trajectories. In total, this study resulted in the collection and classification of 619 bicycle trajectories based on their type of interactions with other road users. The results confirm the success of the proposed methodology in relation to extracting the locations, speeds, and accelerations of the bicycles at a high level of precision. Furthermore, preliminary insights into the acceleration and speed behavior of bicyclists around motorists are determined.

INTRODUCTION

Cycling, as a transportation mode, has been taking an ever-increasing share of the mobility over the last decade. As a sustainable commuting mode, it has been the go-to solution of policymakers to lessen traffic congestion in central downtown areas without further capacity increases. That is justified by the fact that short-distance bike commuting often takes less time when accounting for congestion and delays in public transportation, and presents the most efficient way to increase the road capacity while maintaining existing infrastructure.

Despite the growing interest in bicycle use in the last decade and the urgent need to develop models and planning techniques for bicycle traffic operations, traffic researchers have minimally investigated the traffic flow dynamics of bicycles, unlike vehicular traffic flow, which is heavily studied. The observed literature gap between vehicular and bicycle traffic research is mostly justified by the scarcity, and even the non-existence, of naturalistic cycling data. Most of the existing research that investigated bicycles as a means of transportation [1-6] were in relation to investigating the interactions of bicycles with cars and other possible entities. Technically speaking, a significant portion of those studies falls under, either the Cellular Automata (CA) model that involves discretizing the time and space domain using a non-continuous cell grid such as the work of [1, 2, 4]; or the social force model approach [5, 6] because of its advantages in terms of simulating dynamic lateral dispersion characteristics of mixed traffic. However, while these models offered a concise theoretical framework for the simulation of bicycle longitudinal and lateral traffic behavior in a mixed traffic environment, they were limited in their validation work due to the lack of naturalistic data capturing such interactions.

In addition to the above cycling research that is oriented towards capturing the effect of bicycles in a mixed traffic environment, a few other studies investigated the fundamental concepts behind bicycle longitudinal motion based on the assumption that there are no major differences between the dynamics of single-file bicycle traffic and vehicular traffic. These include models specifically developed for bicycle motion modeling such as the Necessary Deceleration Model (NDM) [7] developed in 2012. Another approach used by researchers to model the longitudinal motion of bicycles investigated the possibility of capturing cyclists'

 doi:10.20944/preprints202209.0275.v1

behavior through revamping certain aspects of existing car-following models. That is the case, for example, in the Intelligent Driver Model (IDM) [8] which, after a simple re-parameterization, was shown to be a good descriptor of bicycle-following behavior [9]. In a similar fashion, driven by the complete overlook of the effects that the cyclist and the road environment have on bicycle motion behavior, the research team proposed a longitudinal motion model for bicycles [10] that is derived from the Fadhloun-Rakha (FR) car-following model [11]. A common factor between the NDM model as well as the proposed IDM and Fadhloun-Rakha bicycle-specific formulations is that they were all validated against cycling data collected in a similar experimental setting in which participants were instructed to follow one another on a ring-road without the possibility of overtaking [7][9]. While the used data in these efforts is in accordance with their assumptions and the approach used is scientifically sound, it is quite clear that those models are not capable of capturing the inherent naturalistic non-lane-based traffic behavior characteristics of bicycles. To address that issue, the research team complemented, in a second stage, the Fadhloun-Rakha longitudinal bicycle-following model with a lateral control module [12], thus inducing a certain degree of freedom in bicycle lateral motion by allowing overtaking maneuvers to occur. However, that effort remained theoretical in nature due to the unavailability of two-dimensional naturalistic cycling data that could serve to validate and verify the model formulation.

While the above studies differed based on their purpose and applications, they all share one key element. That is to say, the complete lack or superficiality of validation work due to the non-existence of naturalistic cycling data that is well fitted for their objectives. In this study, the research team tries to fill, at least partially, the apparent gap in naturalistic data that exist between vehicular traffic and bicycle traffic.

Specifically, this paper describes a research effort that aims to extract naturalistic cycling data from video feeds for use in different mobility applications. To achieve this objective, the research team first applied computer vision, machine learning, and data reduction techniques to a video dataset in order to identify and extract bicycle trips in the pixelated domain of the videos. The selected video dataset is the result of a previous Virginia Tech Transportation Institute study in collaboration with SPIN in which continuous video data at a non-signalized intersection at the Virginia Tech campus was collected. Next, using the results of a high-precision surveying campaign of the observed area, the collected trajectories were projected in the Northing-Easting coordinate system allowing for the determination of the actual locations, speeds, and accelerations of the bicycles. Besides its main contribution that resulted in the collection of 619 bicycle trajectories, it is noteworthy to mention that the trips were classified into different scenarios depending on the type of interactions the bicyclists had with cars. Subsequently, a better understanding of bicyclists' behavior around motorists is achieved. The results could be used to analyze the interactions between cyclists and drivers, both for safety and capacity studies.

Concerning its layout, the paper starts with a brief overview of the used naturalistic video dataset. That is followed with a detailed description of the different methodologies and techniques involved in the extraction of the naturalistic cycling trajectories from the video feeds. Finally, the results and findings of the study are presented.

NATURALISTIC VIDEO DATASET

Due to the continuous proliferation and advancements in machine learning and computer vision techniques, it is becoming feasible to acquire reliable naturalistic traffic data in a cheap and efficient manner from video datasets. That is especially true for the case of bicycles as they are not as instrumented as cars, which would not allow the capture of their full surroundings in the

 doi:10.20944/preprints202209.0275.v1

context of a naturalistic data collection study. In the case of this study, the complete video dataset is the result of a previous Virginia Tech Transportation Institute study in collaboration with SPIN in which continuous video data at several fixed locations at the Virginia Tech campus was collected for a seven-month period. For the purpose of this research, only a portion of the above dataset at a single location is used. The selected dataset was collected over 55 days between the months of September and December 2019 using a roof-mounted high-definition camera facing a non-signalized three-way stop intersection. The selected dataset includes approximately 810 hours of 3720 x 1728 pixels videos recorded at a frequency of 30 Hz. That translates to a total of approximately 87.5 million video frames.

VIDEO PROCESSING

The first step of this research effort involves the identification of the bicycle events from the different videos. Given the big size of the video feed, a manual data reduction was judged to be infeasible, as it will be both a costly and lengthy process. Instead, the research team opted for a more automated route that makes use of existing object detection techniques. Specifically, a two-step object-detection algorithm was developed.

The first step of the proposed algorithm uses a cascade detector based on the histograms of oriented gradients (HOG) with 11 stages to detect potential regions of interest that might be bicycles in the video frames. The number of stages used to train the detector is not random. In fact, the research team initially used a database composed of 400 positive images and 900 negative images to train detectors with different number of stages (5, 7, 9, 11, and 13) and a false alarm rate fixed at 2.5%. The number of training images and stages were purposefully set relatively low in order to ensure a quick training process. The focus of the research team, at this level, was to ensure that the number of stages of the detector is high enough to detect a significant percentage of the true positives regardless of the number of false positives as these will be addressed and eliminated later. Next, the trained detectors were run on a one-hour video from the database at 5-second intervals to quantify their performance. The outputs from this step consisted of bounded areas that highlight regions that might be inclusive of bicycles in the examined video frame, as illustrated in FIGURE 1.

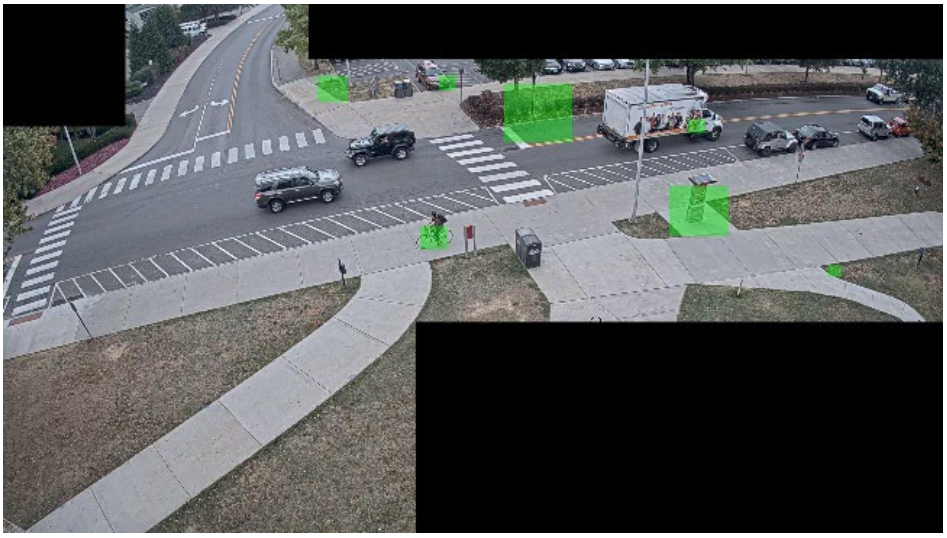

FIGURE 1 Sample output of HOG detectors

 doi:10.20944/preprints202209.0275.v1

The following metrics were used to assist with the evaluation of each of the detectors:

- The number of true positives: These refer to the bounded areas identified correctly by the detectors in that they actually contain a bicycle.
- The number of false positives: These correspond to the bounded areas identified wrongfully by the detectors.
- The number of false negatives: These account for the cases in which a bicycle was present in the video frame without being detected.

It is noteworthy to mention that all the detectors, regardless of their number of stages, were able to identify 42 out of the 44 bicycle trips. However, a deeper look into the results using the above metrics highlighted the huge differences between them. FIGURE 2 plots the variation of the true positives (FIGURE 2.a), false positives (FIGURE 2.b), and false negatives (FIGURE 2.c) against the number of stages used to train the detector. The main revelation from the figures is that the total number of false positives significantly decreases as the number of training stages increases. However, the observed decrease is also accompanied by a decrease in the number of true positives and an increase of the number of false negatives. Based on the observed patterns, it is evident that the detector with 11 stages is the best among those investigated albeit a relatively high number of false positives. To address that issue, the bicycle-detection algorithm was complemented with another technique with the main objective of decreasing the occurrences of false detections.

Preprints (www.preprints.org) | NOT PEER-REVIEWED | Posted: 19 September 2022 doi:10.20944/preprints202209.0275.v1

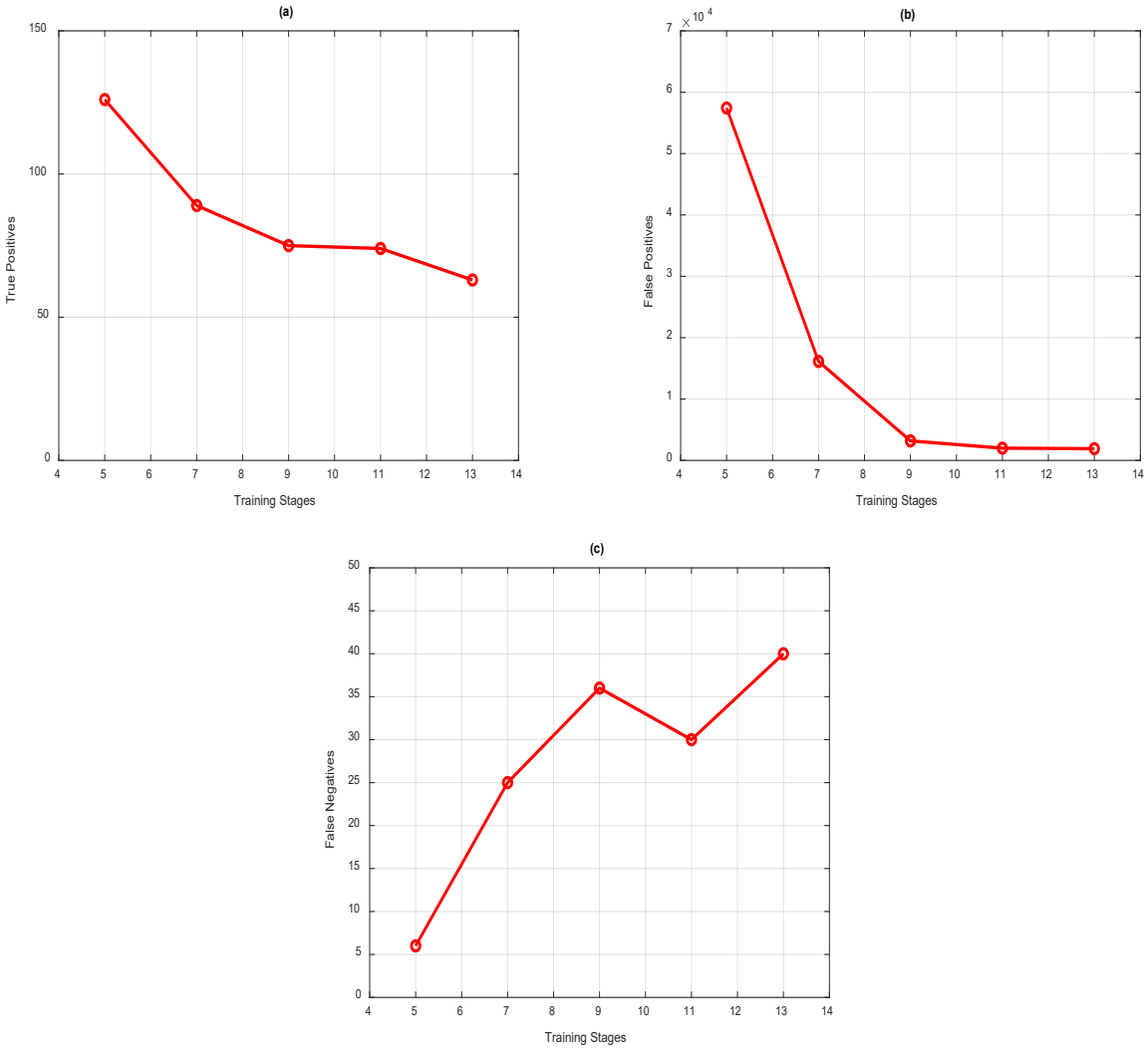

FIGURE 2 Variation of the detector metrics as a function of the number of training stages a) True positives; b) False positives; c) False negatives

In fact, in the second stage of the algorithm, the highlighted areas of interest are selected for further examination using a semantic segmentation network that attempts to classify every pixel in them and assign them to different classes. For that purpose, the research team selected an existing pre-trained DeepLabv3+ network [13], which is a convolutional neural network (CNN) designed for semantic image segmentation. The network is available for download at the Mathworks website and was trained using the CamVid dataset [14] from the University of Cambridge. The dataset consists of a collection of street-level images that are segmented at the pixel-level using 32 semantic classes (such as bicyclist, pedestrian, and car) as shown in FIGURE 3.

 doi:10.20944/preprints202209.0275.v1

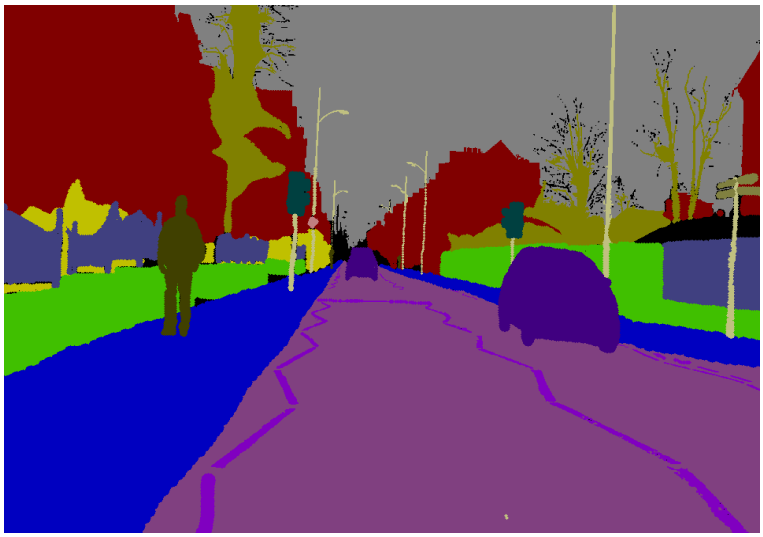

FIGURE 3 Sample image from the CamVid dataset

As mentioned earlier, the main reason behind the semantic segmentation phase is to eliminate the false positives that were detected by the HOG detector in the previous step. That was achieved through a comparison between the number of pixels that were classified as bicyclist and the total number of pixels in the investigated area. If the ratio between the two values is greater than a set threshold of 5% in at least one of the highlighted regions, the examined video frame is saved for manual confirmation. Otherwise, it is rejected (FIGURE 4). The application of the semantic segmentation algorithm over the areas identified by the HOG detector proved to be quite successful. In fact, the number of frames selected for further investigation decreased from 683 frames for the standalone HOG detector to 89 frames when the two algorithms together without any decrease in the number of bicycles detected. The algorithm was able to detect accurately 42 out of the existing 44 bicycle events (95.5%).

With the algorithms ready, the different videos of the database were processed using the HOG detector in conjunction with the semantic segmentation at 5-second intervals. That is mainly due to the heavy computational toll of those algorithms. However, that did not have much effect on the accuracy of the algorithm in bicycle detection as demonstrated earlier. Furthermore, to further illustrate the performance of the algorithm in relation to false positives, it was run on the 4-hour video between 6AM and 10AM on Christmas day, which is a period in which no bicycles were present. The algorithm saved only 21 frames for further investigation out of the 2880 frames examined (< 1%).

FIGURE 4 Sample output after semantic segmentation

EVENT PROCESSING

The previous step resulted in an image database in which the video frames selected for further investigation were saved separately with pertaining information to the date, time, and timestamps in their respective videos. Through a manual data reduction process, the resulting database was investigated to identify the different cycling trips and noting their start times and end times. The end result of this process was the identification of a total of 2259 cycling events.

More importantly, the data reductionists were instructed to classify the identified events based on whether the bicycle interacted with other entities or not during this trip. That is of utmost importance when it comes to validating existing bicycle behavior models. For instance, the portion of trips in which the bicycle is traveling without any impact from the surrounding traffic will be mostly useful for the validation of bicycle motion models (in the free-flow regime where no leader is involved). However, when it comes to mobility studies investigating bicycle interactions with cars (or other modes), information about the interacting entities along with the trajectories of the bicycles is necessary for any validation work.

In that regard, the research team defined 56 scenarios to classify the bicycle trips based on the following criteria. The first criterion relates to the motion behavior of the car. The interacting car with the bicycle is categorized by whether it is moving straight, turning, or coming to a complete stop. The second classification criterion captures the relative position of the bicycle in relation to the car. The bicycle can be behind, ahead, or next to the car. The next criterion looks at whether the bicycle is in the path or out of the path of the car. Finally, the last criterion investigates the relative direction of the bicycle velocity vector in comparison to that of the car. Here, the categorization can take one out of five possible values. The direction of the bicycle velocity vector relative to the car can be either: same, either oncoming, stationary, lateral, or receding.

The definitions of the scenarios along with the total number of events identified for each scenario are presented in TABLE 1. Out of the 2259 events identified by the data reduction team, about 70% (1580) of the trips fall under the first scenario in which the bicycle was traveling independently of other traffic with no observed interactions. It is noteworthy to mention that the predominance of the first scenario is quite understandable given that the Virginia Tech campus is

Preprints (www.preprints.org) | NOT PEER-REVIEWED | Posted: 19 September 2022 doi:10.20944/preprints202209.0275.v1

very cyclable-friendly, and bicycle trips can generally be completed on the sidewalk without having to go on the road. The remaining trips concern scenarios in which interactions did occur. The results show that these are mostly concentrated in four specific scenarios, namely: scenarios 2, 10, 43 and 44. Metrics about the trip durations are presented in FIGURE 5.a and FIGURE 5.b, which illustrate the duration distribution histograms for the trips with no interactions (Scenario 1) and the trips with interactions (remaining scenarios), respectively. The figures confirm that most of the trips have a duration between 10 and 20 seconds with an average of 16.1 seconds and a median of 14.0 seconds.

TABLE 1 Distribution of identified bicycle trips among defined scenarios

Scenario Number	Criteria				Total
	Criteria 1	***Criteria 2***	***Criteria 3***	***Criteria 4***	
1	*No interactions*				1580
2	*Straight*	*Ahead*	*In path*	*Same*	304
3	*Straight*	*Ahead*	*Out of path*	*Same*	13
4	*Straight*	*Ahead*	*In path*	*Oncoming*	7
5	*Straight*	*Ahead*	*Out of path*	*Oncoming*	2
6	*Straight*	*Ahead*	*In path*	*Stationary*	0
7	*Straight*	*Ahead*	*Out of path*	*Stationary*	0
8	*Straight*	*Ahead*	*In path*	*Lateral*	8
9	*Straight*	*Ahead*	*Out of path*	*Lateral*	1
10	*Straight*	*Behind*	*In path*	*Same*	132
11	*Straight*	*Behind*	*Out of path*	*Same*	6
12	*Straight*	*Behind*	*In path*	*Receding*	1
13	*Straight*	*Behind*	*Out of path*	*Receding*	0
14	*Straight*	*Behind*	*In path*	*Stationary*	0
15	*Straight*	*Behind*	*Out of path*	*Stationary*	0
16	*Straight*	*Behind*	*In path*	*Lateral*	1
17	*Straight*	*Behind*	*Out of path*	*Lateral*	0
18	*Straight*	*Next*	*Out of path*	*Same*	12
19	*Straight*	*Next*	*Out of path*	*Receding*	0
20	*Straight*	*Next*	*Out of path*	*Stationary*	0
21	*Straight*	*Next*	*Out of path*	*Lateral*	0
22	*Turning*	*Ahead*	*In path*	*Same*	6
23	*Turning*	*Ahead*	*Out of path*	*Same*	0
24	*Turning*	*Ahead*	*In path*	*Oncoming*	0
25	*Turning*	*Ahead*	*Out of path*	*Oncoming*	1
26	*Turning*	*Ahead*	*In path*	*Stationary*	0
27	*Turning*	*Ahead*	*Out of path*	*Stationary*	0
28	*Turning*	*Behind*	*In path*	*Same*	1
29	*Turning*	*Behind*	*Out of path*	*Same*	0

 doi:10.20944/preprints202209.0275.v1

30	*Turning*	*Behind*	*In path*	*Receding*	0
31	*Turning*	*Behind*	*Out of path*	*Receding*	0
32	*Turning*	*Behind*	*In path*	*Stationary*	0
33	*Turning*	*Behind*	*Out of path*	*Stationary*	1
34	*Turning*	*Next*	*Out of path*	*Same*	0
35	*Turning*	*Next*	*Out of path*	*Receding*	0
36	*Turning*	*Next*	*Out of path*	*Stationary*	0
37	*Stopping*	*Ahead*	*In path*	*Same*	0
38	*Stopping*	*Ahead*	*Out of path*	*Same*	0
39	*Stopping*	*Ahead*	*In path*	*Oncoming*	0
40	*Stopping*	*Ahead*	*Out of path*	*Oncoming*	0
41	*Stopping*	*Ahead*	*In path*	*Stationary*	0
42	*Stopping*	*Ahead*	*Out of path*	*Stationary*	0
43	*Stopping*	*Ahead*	*In path*	*Lateral*	123
44	*Stopping*	*Ahead*	*Out of path*	*Lateral*	60
45	*Stopping*	*Behind*	*In path*	*Same*	0
46	*Stopping*	*Behind*	*Out of path*	*Same*	0
47	*Stopping*	*Behind*	*In path*	*Receding*	0
48	*Stopping*	*Behind*	*Out of path*	*Receding*	0
49	*Stopping*	*Behind*	*In path*	*Stationary*	0
50	*Stopping*	*Behind*	*Out of path*	*Stationary*	0
51	*Stopping*	*Behind*	*In path*	*Lateral*	0
52	*Stopping*	*Behind*	*Out of path*	*Lateral*	0
53	*Stopping*	*Next*	*Out of path*	*Same*	0
54	*Stopping*	*Next*	*Out of path*	*Receding*	0
55	*Stopping*	*Next*	*Out of path*	*Stationary*	0
56	*Stopping*	*Next*	*Out of path*	*Lateral*	0
Total					2259

 doi:10.20944/preprints202209.0275.v1

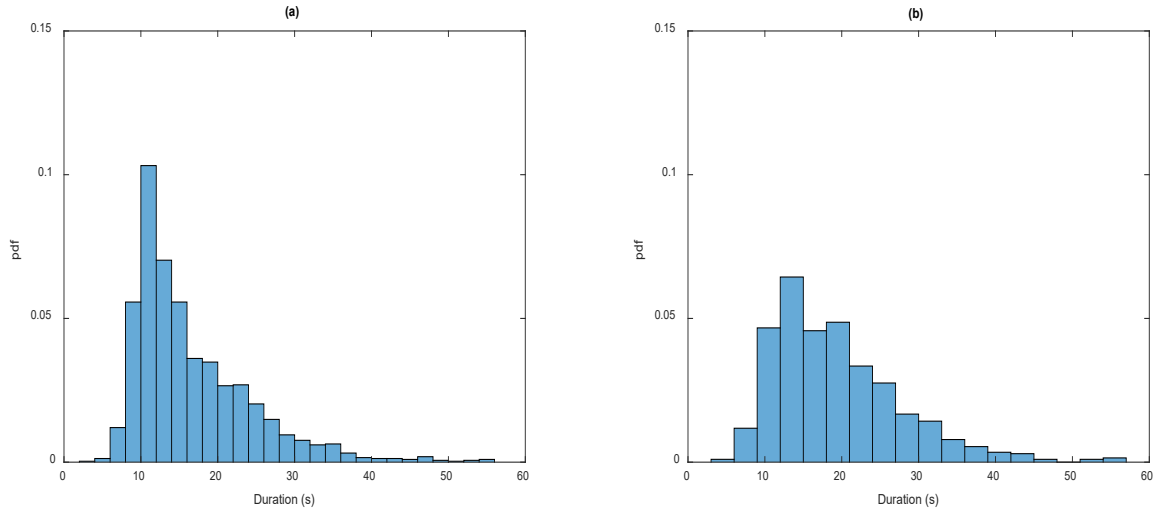

FIGURE 5 Histogram of the duration distribution for a) Trips with no interactions; b) Trips with interactions

TRAJECTORY EXTRACTION

With the start and end times of the different trips known along with identifying information about the type of interactions occurring with motorists, the corresponding video sections are isolated and prepared for the next step, which relates to the extraction of the trajectories in the video pixel domain.

There are two approaches that can be used to achieve the latter. The first approach is quite straightforward but is only possible for a relatively low number of trajectories. For each of the trajectories, a simple script is used to extract the frames from the video at 0.2 seconds allowing for the user to manually click on the position of the bicycle and the vehicles interacting with it. Two moving perpendicular lines are implemented to assist a data reductionist to detect the intersection of the front of the bicycle wheel with the pavement as shown in FIGURE 6. In the background, the script saves the location of the clicks in the (x, y) domain of the video frames (a 3720×1728 pixel grid); thus collecting the trajectories for further processing. It is necessary to note here that if any obstructions interfering with a precise collection of the bicycle location from the video frame exist (such as a car, a tree, or a structure), the bicycle coordinates will not be collected for that specific timeframe. An interpolation algorithm will be used in a later stage to get an estimate at those time steps.

Given that the described process for the extraction of the bicycle trajectories is quite tedious both in relation to the time and cost involved, the research team opted to limit its use, at this time, to the extraction of bicycle trajectories associated with scenarios in which interactions with a vehicle occurred, and for which a significant number of events exists. In that regard, the research team applied the aforementioned process to extract the trajectories falling under scenario 2, 10, 43, and 44. This resulted in the collection of 619 trajectories.

 doi:10.20944/preprints202209.0275.v1

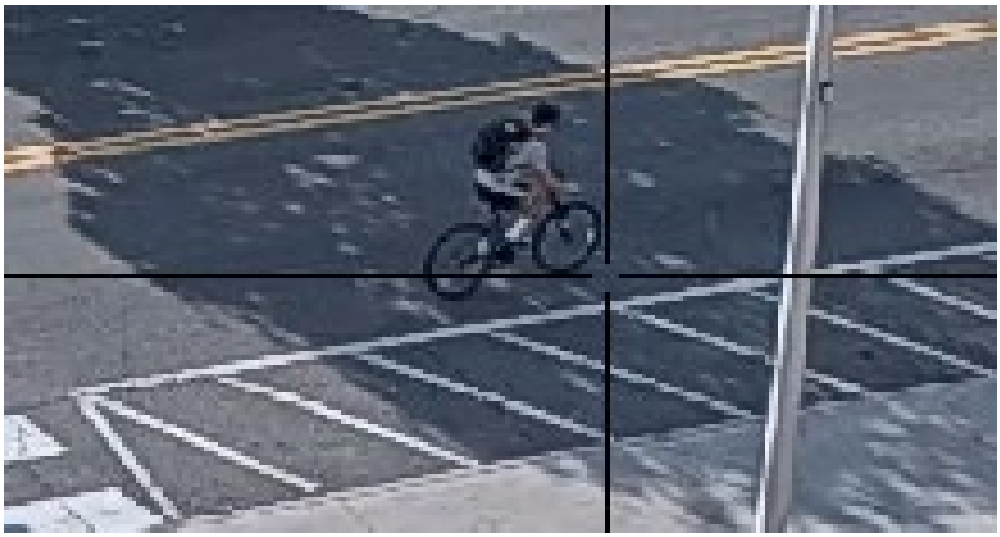

FIGURE 6 Sample screenshot from the trajectory collection process

Before moving on to the description of the next step, we would like to note that our final objective is to extend this work to the extraction of the bicycle trip events that occurred over the entire seven-month period and for all the 14 locations on campus. However, achieving that would require to introduce a certain level of automation to complete the trajectory extraction process. In fact, only 1.2 out of the available 49.5 terabytes of available videos were used so far. Assuming, hypothetically, that a perfect proportionality exists between the number of bicycle trips and the size of the video database, the expected number of trips expected to be found in the entire video dataset would be in excess of 90,000. Even more, once the tasks requiring manual labor are removed, the research community would have access to a comprehensive automated trajectory extraction framework that can be applied to similar videos.

In that regard, the research team is currently working on developing an automated tool for the extraction of the trajectories that can replace the data reduction process. Without going into much detail as this is still a work in progress, the concept of the algorithm consists of using the Hough transform for the detection of bicycle wheels allowing the determination of their contact point with the road surface. To achieve that, edge detection techniques are first used to isolate the bicycle trip on a black and white background as shown in FIGURE 7. After that, Hough transform is used to detect the wheels as shown in FIGURE 8. However, the research team is currently still working on solving the most challenging part of this process, which deals with the fine-tuning of the algorithm in relation to the assignment of the detected points to their corresponding trajectories and the automatic exclusion of false positives.

Preprints (www.preprints.org) | NOT PEER-REVIEWED | Posted: 19 September 2022 doi:10.20944/preprints202209.0275.v1

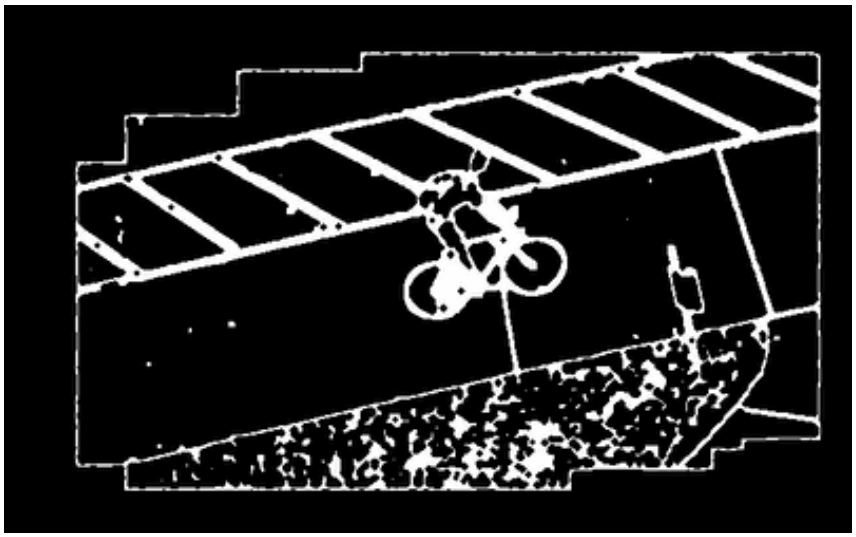

FIGURE 7 Image filtering using edge detection techniques

FIGURE 8 Detection of bicycle wheels using Hough transform

INTERSECTION SURVEYING

In order to convert the extracted trajectories into naturalistic trajectories, a grid map overlay of GPS coordinates at specific locations, which are easily identifiable both in the video frames and in the field, is needed. In fact, the aforementioned map is the element that would allow the conversion of the pixel-based trajectories into distance-based trajectories using the multi-step algorithm described thereafter.

To achieve the stated objective, the research team started by creating a mesh of approximately 400 points as shown in FIGURE 9. As the figure shows, the points are heavily concentrated around the edges of the sidewalks and the road crossings because they are the easiest to identify in the videos as well as in the field. That is quite useful for the next step as both the sidewalks and the road crossings are the most used by the bicyclists to complete their trips. Initial attempts to collect the GPS coordinates at the specified locations were made using accessible tools such as Google Earth and existing GPS mobile applications. However, those

 doi:10.20944/preprints202209.0275.v1

attempts proved unsuccessful due to the small distances involved and the relative low accuracy of those tools when used in this context. As a result, a surveying campaign using professional high-precision tools was conducted to acquire the required coordinates, which are expressed in the Northing-Easting-Elevation coordinates system. Since the investigated area is relatively flat, the elevation data can be ignored without major repercussions on the results. In what follows, we will refer to the data collected in this step by the transform matrix.

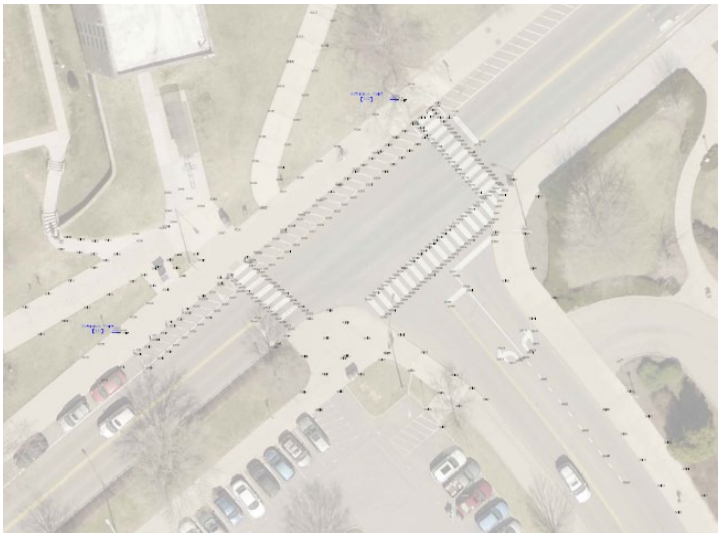

FIGURE 9 An aerial view of the surveyed area and the collection points

TRAJECTORY TRANSFORMATION AND RESULTS

The final phase in this research deals with the conversion of the extracted trajectories that are currently expressed in the video pixel domain to actual naturalistic trajectories allowing access to the distances traveled along with the associated speed and acceleration profiles. That would constitute the final product of this study and would allow traffic researchers to validate their theories and models against the resulting naturalistic bicyclist dataset. The trajectory transformation process is achieved using the following multi-step algorithm:

1. A linear interpolation algorithm is used initially to complement the extracted trajectories with estimated values at the level of the time steps for which the determination of the bicycle location was impossible due to the presence of visual obstructions.
2. Next, the trajectories are exponentially smoothed using a smoothing factor of 0.5. The purpose of the exponential smoothing operation is to address the noise and the zigzag-like features that might be present as a result of the manual trajectory extraction process. At this level, the trajectories will look similar to the two sample trajectories presented in FIGURE 10.
3. For each of the observations composing a trajectory, one of the closest convex hulls containing the observation and delimited by three points from the transform matrix is identified.
4. Since we have access to the coordinates of the points defining the convex hull in both coordinate systems, the coordinates of the trajectory observation could be approximated in the Northing-Easting coordinate system using a triangulation algorithm.

 doi:10.20944/preprints202209.0275.v1

5. Once Step 4 is completed for all the observations, the speed profile associated with the obtained trajectory is determined and smoothed through the application of a third order Savitzky–Golay filter.
6. In a similar fashion to Step 5, the acceleration profile is obtained from the smoothed speed profile and smoothed using a similar Savitzky–Golay filter.
7. The speed profile, the distance traveled, and the coordinates of the trajectory in the Northing-Easting coordinate system are updated backwards to account for the effect of the two-layer filtering that was applied.

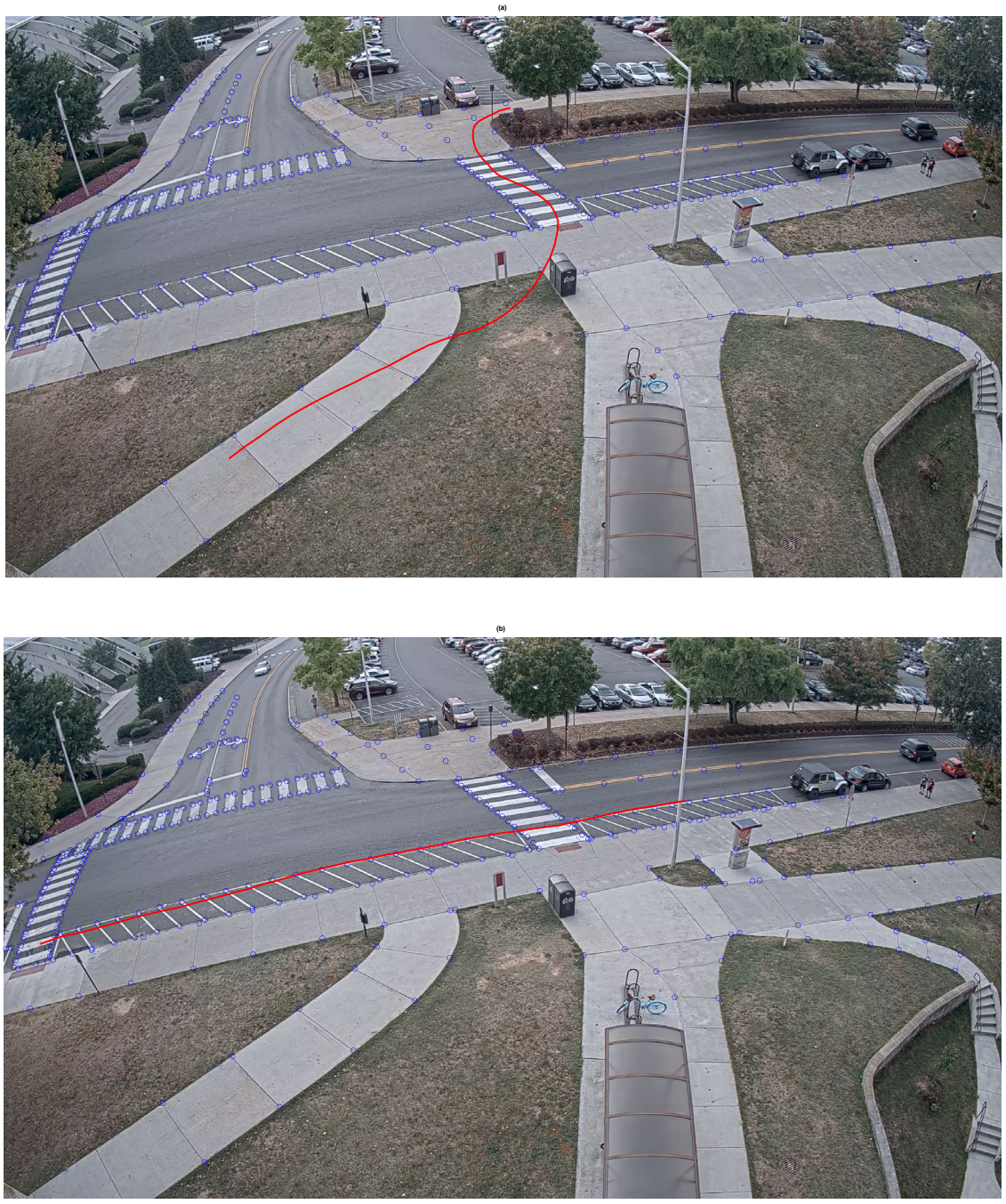

FIGURE 10 Sample trajectories in the video pixel domain

Preprints (www.preprints.org) | NOT PEER-REVIEWED | Posted: 19 September 2022 doi:10.20944/preprints202209.0275.v1

Sample results from this step are presented in FIGURE 11 and FIGURE 12. FIGURE 11 shows the resulting trajectories in the Northing-Easting coordinate system corresponding to the two trajectories presented in FIGURE 10. The figure demonstrates the success of the proposed multi-step algorithm in conserving the shape and main features of the extracted trajectory. Meanwhile, FIGURE 12 illustrates the distance traveled, speed, and acceleration profiles corresponding to the trajectory presented in FIGURE 10.a and FIGURE 11.a.

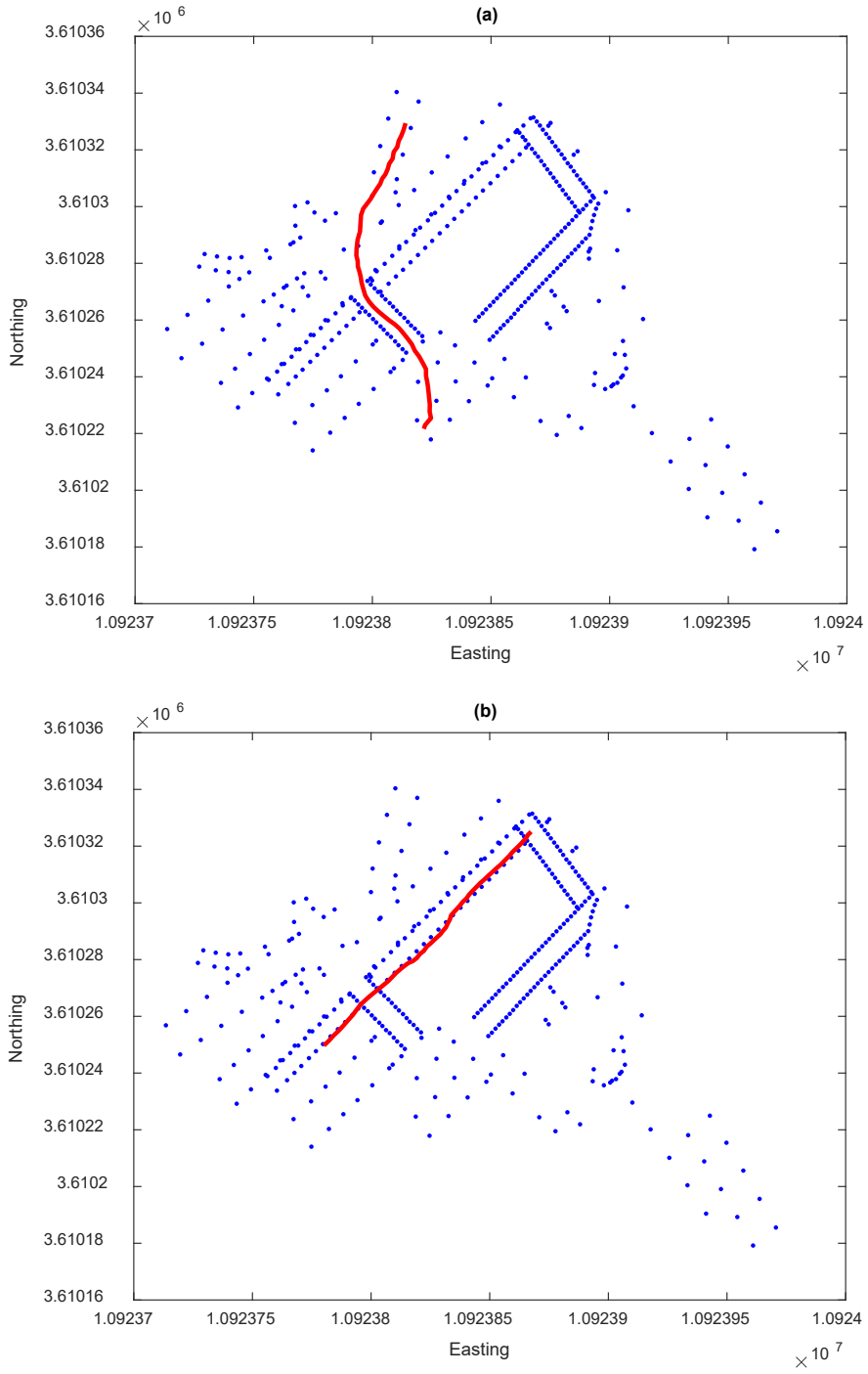

FIGURE 11 Sample naturalistic trajectories after the triangulation procedure

Preprints (www.preprints.org) | NOT PEER-REVIEWED | Posted: 19 September 2022 doi:10.20944/preprints202209.0275.v1

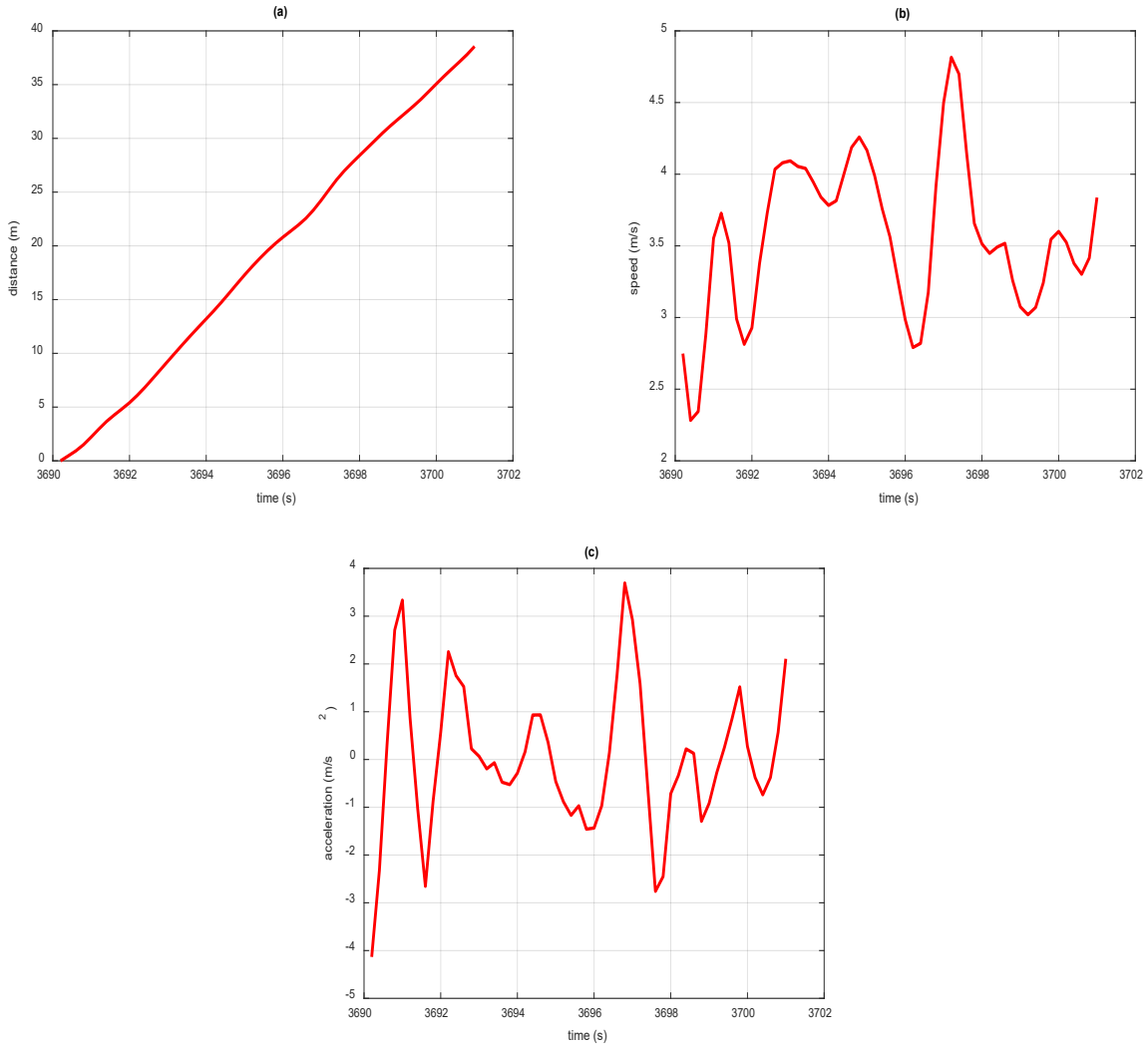

FIGURE 12 Extraction of the distance traveled, speed, and acceleration profiles for a naturalistic trajectory a) Distance traveled; b) Speed profile; c) Acceleration profile

Finally, the histograms of the instantaneous accelerations and speeds from all the 619 trajectories is investigated to confirm the consistency of the obtained values with bicycle behavior. The results, which are plotted in FIGURE 13, show that the results are concentrated around low acceleration levels and speeds that are quite typical for bicyclists. Furthermore, the range of the observed values can be confirmed to be physically feasible for a bicycle. A deeper look at the results is possible by looking at the histograms corresponding to each of the four investigated scenarios. The results are presented in FIGURE 14 (for Scenario 2), FIGURE 15 (for Scenario 10), FIGURE 16 (for Scenario 43), and FIGURE 17 (for Scenario 44). The aforementioned figures confirm the ability of the resulting trajectory dataset to capture the effect of the type of interaction on bicyclists' speed and acceleration behavior. This can lead to a better understanding of bicyclists' behavior around cars and can prove very useful for a multitude of studies such as safety analysis research.

Preprints (www.preprints.org) | NOT PEER-REVIEWED | Posted: 19 September 2022 doi:10.20944/preprints202209.0275.v1

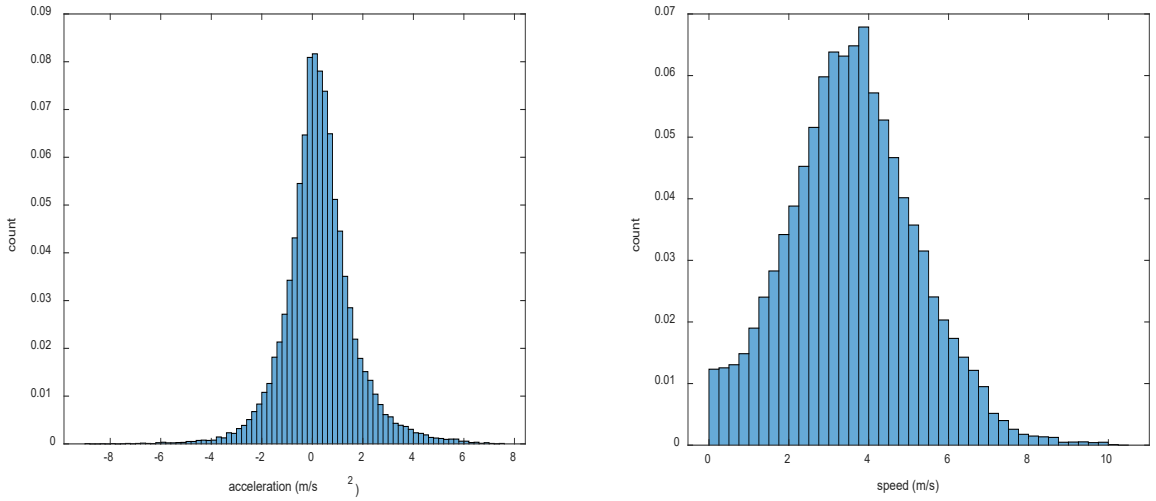

FIGURE 13 Histogram of the instantaneous accelerations and speeds of the aggregated extracted trajectories

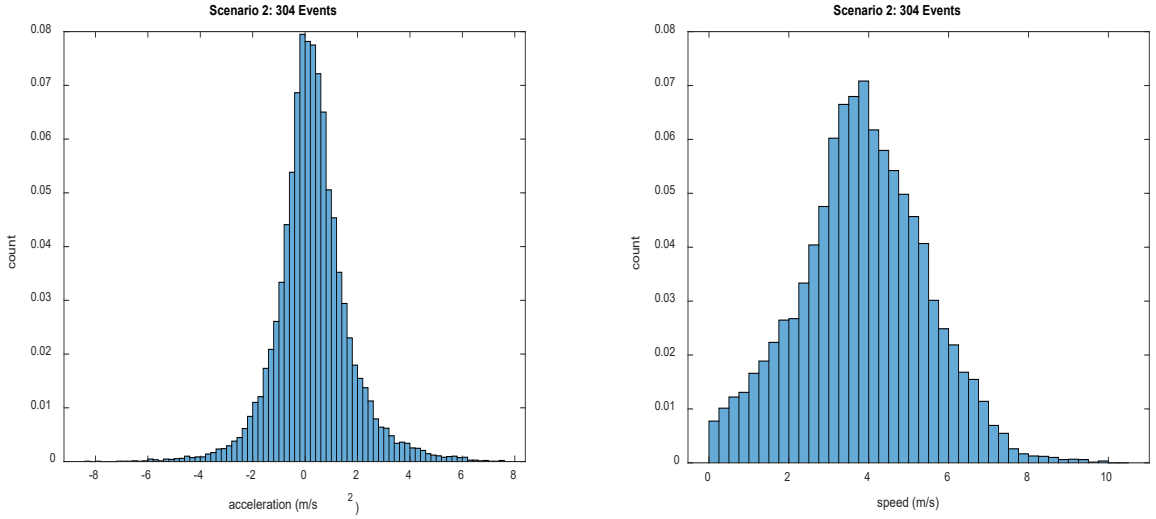

FIGURE 14 Histogram of the instantaneous accelerations and speeds of the extracted trajectories corresponding to Scenario 2

Preprints (www.preprints.org) | NOT PEER-REVIEWED | Posted: 19 September 2022 doi:10.20944/preprints202209.0275.v1

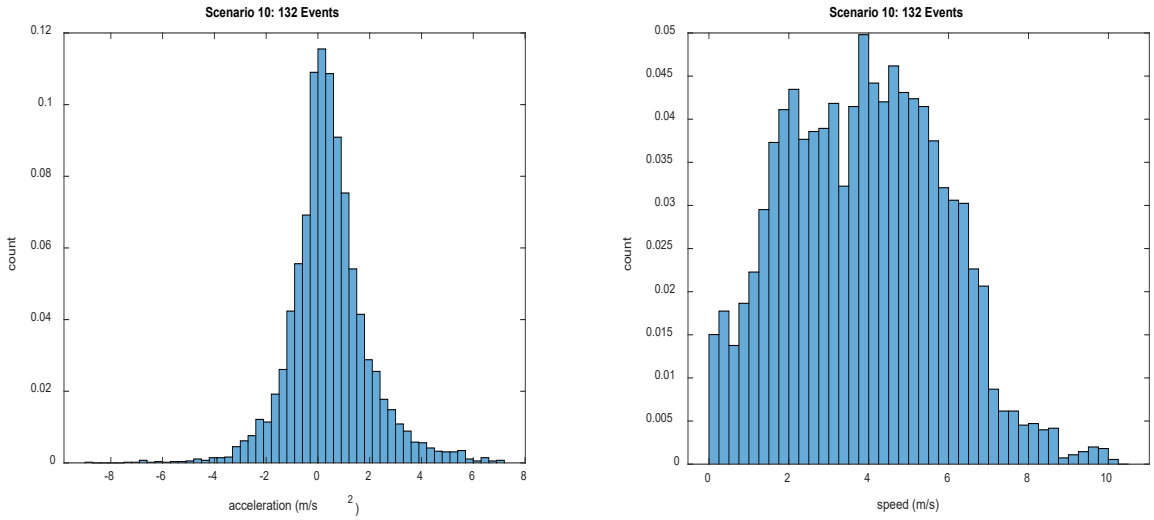

FIGURE 15 Histogram of the instantaneous accelerations and speeds of the extracted trajectories corresponding to Scenario 10

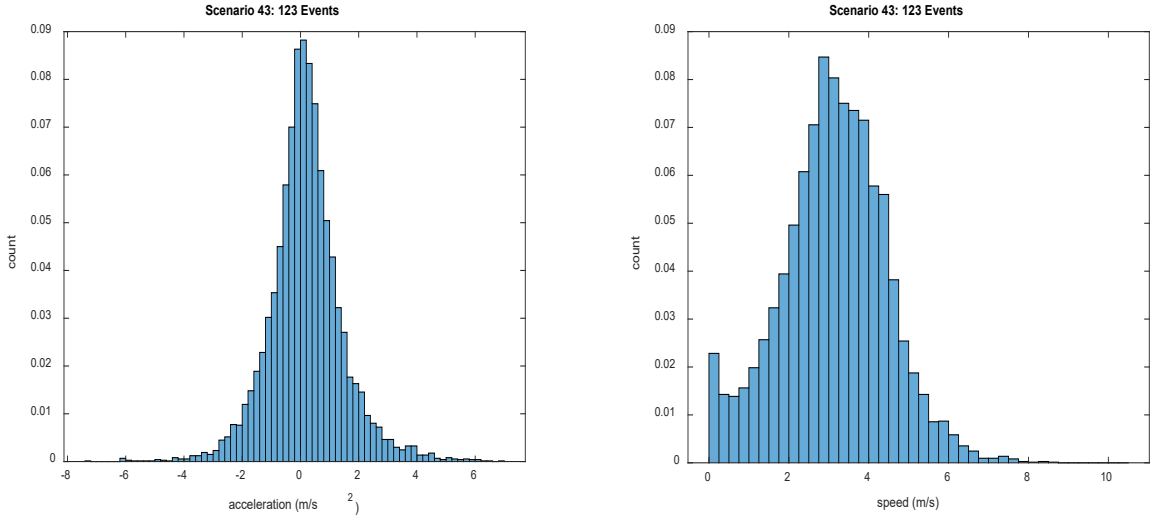

FIGURE 16 Histogram of the instantaneous accelerations and speeds of the extracted trajectories corresponding to Scenario 43

Preprints (www.preprints.org) | NOT PEER-REVIEWED | Posted: 19 September 2022 doi:10.20944/preprints202209.0275.v1

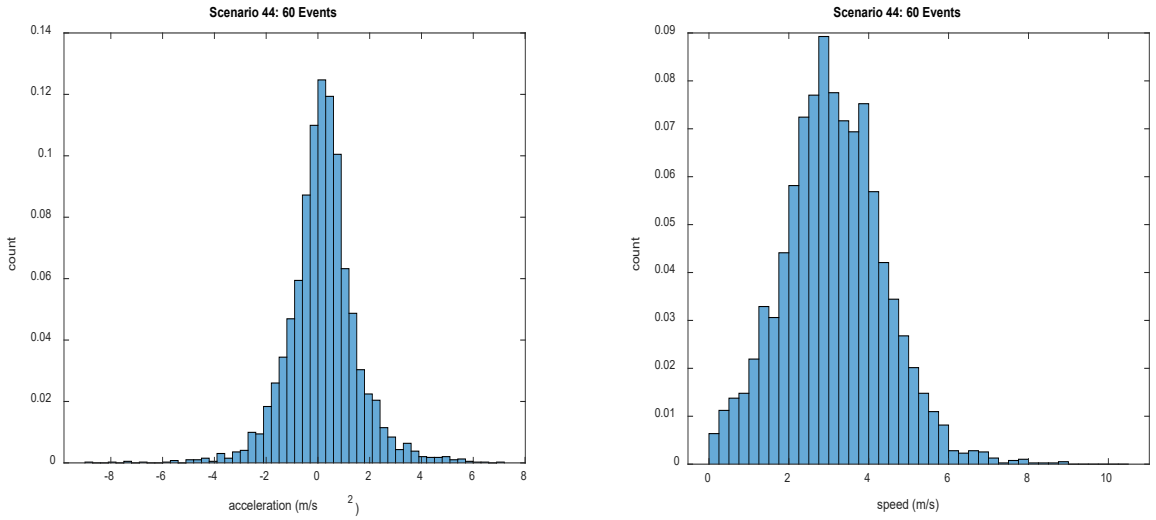

FIGURE 17 Histogram of the instantaneous accelerations and speeds of the extracted trajectories corresponding to Scenario 44

CONCLUSIONS AND FUTURE WORK

In the context of a better understanding of bicyclists' behavior, this paper described the development of a comprehensive framework that would allow for the collection of naturalistic cycling trajectories from video feeds. Even though the current naturalistic dataset is composed of only 619 trajectories, it will be useful to traffic researchers in several mobility applications such as the validation of studies investigating bicycle motion behavior such as the model [12] developed by the research team. Furthermore, the collected trajectories will contribute to a better understanding of bicyclists' behavior around cars leading to a better understanding of the interactions between bicycles and other modes of transportation. More importantly, the significance of this work will be further accentuated once the trajectories of the cars and other entities interacting with the bicycles is extracted.

The research team faced two main challenges during this study. The first challenge deals with automating the process of extracting the bicycle trajectories from the videos through the detection of bicycle wheels. In fact, the number of trajectories in the resulting dataset is limited due to the problems encountered while trying to complete that process. Once those problems are addressed, the size of the trajectory database will increase significantly. More importantly, the proposed methodology will be completely transferable for use by other researchers at different locations. The second challenge relates to the collection of the transform matrix needed to transform the video trajectories into actual trajectories. Due to the small distances involved, typical tools such as Google Maps and existing GPS applications cannot be used; instead, a professional surveying campaign of the observed area is needed.

Overall, the proposed framework for the extraction of bicycle trajectories from big video datasets is demonstrated to be comprehensive and accurate. The findings seem to be consistent with actual bicycle behavior, which is generally characterized by low acceleration levels. As a future work, the research team plans to continue extending this dataset and complement it with the trajectories of the entities interacting with the bicycles. Once that is achieved, this work will result in the most complete naturalistic dataset that, not only include data relevant to the bicycle, but also information about any vehicles or entities that had an influence on its behavior.

ACKNOWLEDGMENTS

The authors acknowledge the financial support provided by the University Mobility and Equity Center (UMEC) and funding from the Ford Motor Company.

AUTHOR CONTRIBUTIONS

The authors confirm contribution to the paper as follows: study conception and design: Rakha, Fadhloun and Mittal; data collection: Alazemi and Fadhloun; analysis and interpretation of results: Alazemi, Fadhloun, and Rakha; draft manuscript preparation: Alazemi, Fadhloun, Rakha, and Mittal. All authors reviewed the results and approved the final version of the manuscript.

REFERENCES

1. Jia, B., et al., *Multi-value cellular automata model for mixed bicycle flow.* The European Physical Journal B, 2007. **56**(3): p. 247-252.
2. Jiang, H., et al., *Evaluation of the dispersion effect in through movement bicycles at signalized intersection via cellular automata simulation.* 2018. **498**: p. 138-147.
3. Jiang, R., et al., *Traffic dynamics of bicycle flow: experiment and modeling.* 2017. **51**(3): p. 998-1008.
4. Ren, G., et al., *Heterogeneous cellular automata model for straight-through bicycle traffic at signalized intersection.* 2016. **451**: p. 70-83.
5. Qu, Z.-w., et al., *Modeling electric bike–car mixed flow via social force model.* 2017. **9**(9): p. 1687814017719641.
6. Li, Y., et al., *A modified social force model for high-density through bicycle flow at mixed-traffic intersections.* 2021. **108**: p. 102265.
7. Andresen, E., et al. *Basic Driving Dynamics of Cyclists*. 2014. Berlin, Heidelberg: Springer Berlin Heidelberg.
8. Treiber, M., A. Hennecke, and D. Helbing, *Congested traffic states in empirical observations and microscopic simulations.* Physical review E, 2000. **62**(2): p. 1805.
9. Kurtc, V. and M. Treiber, *Simulating bicycle traffic by the intelligent-driver model-Reproducing the traffic-wave characteristics observed in a bicycle-following experiment.* Journal of Traffic and Transportation Engineering (English Edition), 2020.
10. Fadhloun, K.R., Hesham; Mittal, Archak, *Bicycle Longitudinal Motion Modeling.* 100th Annual Meeting Transportation Research Board, 2021.
11. Fadhloun, K. and H. Rakha, *A novel vehicle dynamics and human behavior car-following model: model development and preliminary testing.* International journal of transportation science and technology, 2020. **9**(1): p. 14-28.
12. Alazemi, F.F., Karim; Rakha, Hesham; Mittal, Archak, *An Entropy-based Dynamics Model for Bicycle Longitudinal and Lateral Motion Modeling*, in *101th Annual Meeting Transportation Research Board*. 2022.
13. Chen, L.-C., et al. *Encoder-decoder with atrous separable convolution for semantic image segmentation*. in *Proceedings of the European conference on computer vision (ECCV)*. 2018.
14. Brostow, G.J., J. Fauqueur, and R.J.P.R.L. Cipolla, *Semantic object classes in video: A high-definition ground truth database.* 2009. **30**(2): p. 88-97.